Rapid Green Manufacture of High Yield CdTe@$Ca(OH)_2$ Nanocrystals and Their Performance on WLED

Zhixing Zhao, Xiao-Qiao Wang, Luting Ling, Cai-Feng Wang, and Su Chen
State Key Laboratory of Materials-Oriented Chemical Engineering, College of Chemistry and Chemical Engineering, Nanjing Tech University, No. 5 Xin Mofan Road, Nanjing 210009, P.R. China

DOI 10.1002/aic.15133
Published online December 25, 2015 in Wiley Online Library (wileyonlinelibrary.com)

The bottleneck of large-scale production of semiconductor quantum dots (QDs) is how to solve heavy metal ions waste water and the rapid separation during industrial process. A facile strategy for fabricating CdTe@$Ca(OH)_2$ nanocrystals exhibiting both improved photoluminescence (PL) stability and prolonged PL lifetime via an economical coprecipitating technology is reported herein. The procedure on capping CdTe QDs into $Ca(OH)_2$ crystals can enable the products to be easily filtrating separation and the content of residual Cd^{2+} filtrate solution to be reached to 0.238 ppm level. Also, fluorescent rod-like heterocrystals by addition of saturated $CaCl_2$ solution is constructed. CdTe@$Ca(OH)_2$ nanocrystals is utilized further as phosphor powders to construct white light emitting diode (WLED). The WLED presented, here, has good photoelectric properties with color rendering index of 82.4 at 350 mA, a color temperature of 4643 k, and Commission Internationale de L'Eclairage coordinate of (0.3548, 0.3532), belonging to the white gamut, showing great potential in industrial application. *AIChE J*, 62: 580–588, 2016
Keywords: quantum dot, nanocrystal, CdTe@$Ca(OH)_2$, photoluminescence stability, white light emitting diode

Introduction

Semiconductor nanocrystals, known as quantum dots (QDs), have attracted the researchers' interest owing to their unique quantum confinement effect and quantum size effect,[1–4] which are applied in optics,[5] electroluminescent devices,[6,7] fluorescent tags,[1,8] and photovoltaic cells.[9] Among QDs, the II-VI semiconductor QDs, such as water-soluble CdS, CdTe, ZnTe, and ZnS, are the most common QDs due to their various applications.[10–17] However, in most cases, the solid content of water-soluble QDs is normally less than 0.5 wt %, leading to a number of heavy metal ions toxic waste water and hard separation of QDs powder from these solutions. So far, the production of II-VI semiconductor QDs powder is still costly, time consuming, environmentally unfriendly, and low output, impeding their large-scale industrial applications. To solve it, much effort has been developed by designing core/shell structural QDs, such as CdTe/ZnS, CdTe/ZnSe, or CdTe/ZnTe core/shell QDs and the like.[18–20] Another solution is that some approaches adopted stable inorganic compounds to encapsulate QDs, further enhancing their stability of as-prepared QDs.[21–25] Although the progresses have been made, the as-generated toxic heavy metal ions waste water still exists during the producing process, along with harsh separation of QDs powder, limiting their extensive industrialization of QDs.

In this work, we demonstrate a strategy to generate CdTe@-$Ca(OH)_2$ powders with high yield and robust stability, which is performed capping CdTe QDs into $Ca(OH)_2$ crystals via a coprecipitation method (seen in Scheme 1). This method is of the following advantages: (1) this robust procedure allows the residual concentration of Cd^{2+} ions in water-soluble CdTe QDs solution to be dramatically decreased from 1843.45 mg/L to 0.238 mg/L after CdTe QDs being capped by $Ca(OH)_2$ crystals, making it possible to realize relatively green synthesis of water-soluble QDs; (2) easily rapid separation of QDs powder from original solutions with high efficiency and yield via a simple filtration; (3) after $Ca(OH)_2$ crystal capping CdTe QDs, the thermostability of CdTe@$Ca(OH)_2$ nanocrystals was highly enhanced and the photoluminescence (PL) lifetime was also greatly prolonged. We further construct fluorescent rod-like heterocrystals by dispersing CdTe@$Ca(OH)_2$ nanocrystals into saturated $CaCl_2$ solution. For more practice, we applied CdTe@$Ca(OH)_2$ powders as phosphors to construct white light emitting diode (WLED). The as-fabricated WLED shows ideal photoelectric properties with a color rendering index (CRI) of 82.4 at 350 mA, a color temperature of 4643 K and Commission Internationale de L'Eclairage (CIE) coordinate of (0.3548, 0.3532), which belongs to the white gamut. Therefore, this finding might open an available pathway to green synthesis of high performance QDs powder, along with facile technology advantage.

Experimental

Materials

Cadmium chloride hemipentahydrate ($CdCl_2 \cdot 2.5\ H_2O$) was purchased from Alfa Aesar. N-acetyl-L-systeine (NAC), ethanol and sodium borohydride ($NaBH_4$) were supplied by Sinopharm Chemical Reagent (Shanghai, China). Sodium

Correspondence concerning this article should be addressed to S. Chen at chensu@njtech.edu.cn.

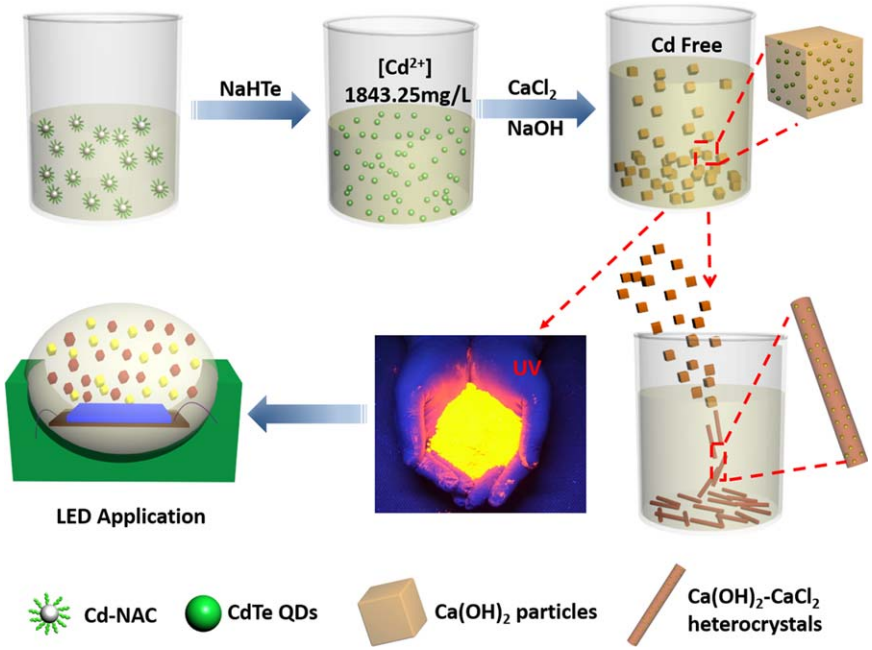

Scheme 1. Synthesis, regrowth and application of CdTe@$Ca(OH)_2$ nanocrystals.

[Color figure can be viewed in the online issue, which is available at wileyonlinelibrary.com.]

hydroxide (NaOH), calcium chloride dehydrate ($CaCl_2{\cdot}2H_2O$), tellurium powder were purchased from Aladdin. All the materials were used as received without further purification.

Synthesis of fresh oxygen-free NaHTe

The sodium hydrogen telluride was prepared similar to our previous work.[26] Typically, tellurium powder (191.4 mg, 1.5 mmol) was added to a 5 mL vial loaded with $NaBH_4$ (68.1 mg, 1.8 mmol) and 4 mL water. After sealing the vial, an outlet was connected with the vial to release the hydrogen generated during the reaction. The vial was kept in an ice-water bath for 8 h.

Preparation of water-soluble CdTe QDs stock solution

Water-soluble CdTe QDs capped with NAC was prepared according to previous literatures with little modification.[27,28] 733.6 mg (4.5 mmol) NAC dissolved in 20 mL DI water was poured into a three-necked flask containing 150 mL 0.02 M $CdCl_2$. Then 5 M NaOH was added to adjust the pH value to 9.0. Nitrogen gas was bubble into the solution to remove oxygen gas. The NaHTe solution was injected into the solution when the temperature was raised to 95°C. After refluxing at 95°C for different time, CdTe QDs with different sizes were done. Aliquots were taken by a syringe to monitor the reaction. When the synthesis of CdTe QDs was done, the temperature of the solution was cooled to room temperature, and then to terminate the reaction. This solution was used as stock solution without further purification.

Incorporation of CdTe QDs into calcium hydroxide crystals

In a typical synthesis, 2 mL 4 M $CaCl_2$ solution and 16 mL CdTe QDs stock solution were mixed in a vial, then 2 mL 8 M NaOH solution was added dropwise into the vial under vigorous stirring. Consequently, we obtained 20 mL turbid liquid containing 0.4 M $Ca(OH)_2$ and diluted CdTe QDs. Filtering the turbid liquid by the filter membrane and washing the obtained powders with ethanol to wash away the unreacted chemicals. Moving the filter membrane loaded with the powders to vacuum drying oven to dry the powders. In this case, the QDs were used as obtained without further dilution or purification. Varying the emission wavelength of the QDs used and changing the concentration of $CaCl_2$ and NaOH proportionally according to their stoichiometry to obtain different concentrations of $Ca(OH)_2$ encapsulated with QDs emitting from green to red. For simplification, the NAC-CdTe QDs embedded $Ca(OH)_2$ crystals are designated as CdTe@$Ca(OH)_2$.

Growth of the CdTe@$Ca(OH)_2$ nanocrystals into fluorescent rod-like heterocrystals

Two gram of dried CdTe@$Ca(OH)_2$ nanocrystals were further soaked in 10 mL saturated $CaCl_2$ solution to synthesize heterocrystals which consisted of CdTe QDs embedded with $Ca(OH)_2$ and a small amount of $CaCl_2$. The PL maximum emission peak of CdTe@$Ca(OH)_2$ (0.4 M) was 575 nm. After half an hour, heterocrystals were obtained by filtering separation, and then washed with ethanol for several times and dried under atmosphere.

Thermostability test

In a typical run, part of the dried QDs powder with an emission peak maximum of 631 nm was used to synthesize QDs embedded 0.4 M $Ca(OH)_2$, another part of the dried QDs powder was used as control sample. The obtained CdTe@$Ca(OH)_2$ nanocrystals and the pure QDs were put in the tube furnace. Both of the two samples were kept in the tube furnace at 150°C for 1 h. Testing the PL spectra of the two samples and comparing them with the unheated samples, respectively.

Preparation of the WLED

The CdTe@$Ca(OH)_2$ nanocrystals were used as phosphors to fabricate WLED. A UV-LED chip, emitting at 450 nm, was attached on the bottom of the reflector cup by using conductive silver paste. In a typical procedure, 0.5 g 0.4 M

$CdTe@Ca(OH)_2$ nanocrystals with peak wavelength centered at 560 nm were mixed with 0.5 g 0.4 M $CdTe@Ca(OH)_2$ nanocrystals emitting at 625 nm, then mixing them with 1 g silicone at the weight ratio of 0.5:0.5:1 (OE-6550A:OE-6550B) according to our previously reported method.[29] Removing the bubbles and solvent in the resin in a vacuum chamber and overcoating the mixture of silicone and nanophosphors on the chip. After that, the chip was cured at 150°C for 60 min. Afterward, capping the reflector cup with an optical lens and filling the void with transparent silicone. To obtain the final product, the LED was cured at 150°C for 1 h again.

Characterization

The morphology of the $CdTe@Ca(OH)_2$ nanocrystals were observed by scanning electron microscopy (SEM) with a QUANTA 200 (Philips-FEI, Holland) instrument at 5.0 kV. The energy dispersive X-ray (EDX) analysis of the $CdTe@Ca(OH)_2$ nanocrystals was also obtained by SEM. The fluorescent images of the $CdTe@Ca(OH)_2$ nanocrystals were taken by a Zeiss AXIO 5 Imager optical microscope. All of the PL spectra, except the PL spectrum of the rod-like heterocrystals, were measured by a Varian Cary Eclipse spectrophotometer at room temperature operating with a 390 nm laser beam as a light source and Xe lamp as excited source. The PL spectrum of the rod-like heterocrystals was measured by Leica TCS/SP2 confocal microscope system. The X-ray diffraction (XRD) pattern was conducted on a Bruker-AXS D8 ADVANCE X-ray diffractometer with Cu-Kα radiation ($\lambda = 0.1542$ nm) at a scanning speed of 10°/min over 2θ range of 5°–80°. The concentrations of cadmium were determined by a Perkin-Elmer Optima 2000 DV optical emission spectrometer. The time-resolved PL decay curves were obtained based on the time-correlated single-photon counting via a SPC-830 module. All the optical parameters of LEDs were measured by a ZWL-600 Spectral Radiation Analyzer with an integrating sphere at room temperature.

Results and Discussion

Synthesis and characterization of the NAC-CdTe QDs and $CdTe@Ca(OH)_2$ nanocrystals

The synthesis of $CdTe@Ca(OH)_2$ nanocrystals started from preparation of NAC-CdTe QDs. First, the water soluble NAC capped CdTe QDs were prepared using Cd^{2+} and HTe^- solutions for refluxing several hours according to previous literatures.[27,28] As the prolongation of refluxing time, the color of the solution changed from light red to deep red. The TEM (Transmission Electron Microscopy) result of the CdTe QDs sample obtained by refluxing for 180 min is shown in Figure 1a. As shown in Figure 1a, the as-prepared CdTe QDs are well dispersed, along with distinct lattice fringes and average particle size of 3–4 nm. The high resolution TEM (HRTEM inset in Figure 1a) presents the interplanar distance of this QD is about 0.38 nm, which is correspond to the (111) plane of cubic CdTe (JCPDS Card No. 15-0770). From powder XRD measurement (Figure 1b), the crystalline diffraction peaks of CdTe QDs at 2θ are noted at 23.8°, 40.2°, and 46.7°, corresponding to the (111), (220), and (311) planes of cubic CdTe structure.[30,31] The peaks are weak and wide, implying the size of the QDs is small.[31] The histogram of the QDs size distribution (Figure 1d), calculated based on measuring the sizes of QDs in Figure 1c, shows that the QDs have a narrow size distribution

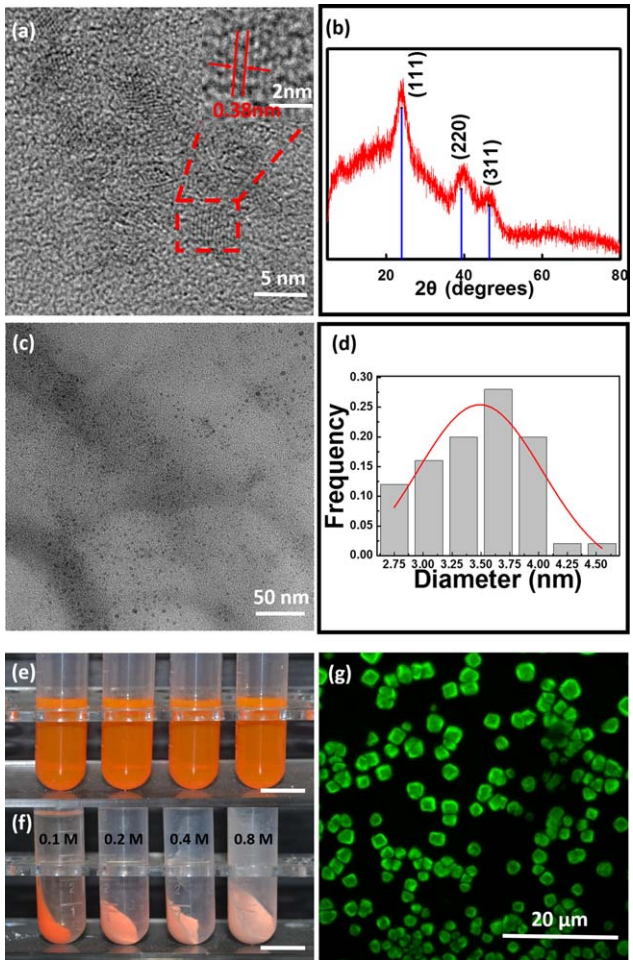

Figure 1. (a) TEM image of NAC-CdTe QDs obtained by refluxing for 180 min. Inset: HRTEM image of the QD; (b) XRD pattern of NAC-CdTe QDs; (c) Low resolution TEM image of NAC-CdTe QDs obtained by refluxing for 180 min; (d) Histogram of the QDs size distribution measured from (c); (e) digital image of CdTe QDs solution; (f) digital image of $CdTe@Ca(OH)_2$ crystals. The scale bars (e and f) are both 1 cm; (g) fluorescent microscope image of $CdTe@Ca(OH)_2$ ($Ca(OH)_2 = 0.4$ M) nanocrystals.

[Color figure can be viewed in the online issue, which is available at wileyonlinelibrary.com.]

with average size of 3.5 nm. The XRD and TEM results have confirmed the successful synthesis of well-defined CdTe QDs. The digital image of QDs solution shown in Figure 1e displays it presents transparent because of their smaller particle sizes (<5 nm) and lower solid content (<0.5 wt %).

Previously, the separation to this kind of QDs powder is highly replied on costly centrifugal machine along with more than 10,000 rpm revolving speed.[32] Also, after centrifugation, the residual heavy metal ions liquid still exists in the filtrate. This traditional separation model cannot enable them to be further scaled up in the industry. We herein added correspondingly different concentrations of $CaCl_2$ (0.1, 0.2, 0.4, and 0.8 M) and NaOH (0.2, 0.4, 0.8, and 1.6 M) solutions to the QDs stock solution, and consequently a series of $CdTe@Ca(OH)_2$ powders with different concentrations of $Ca(OH)_2$

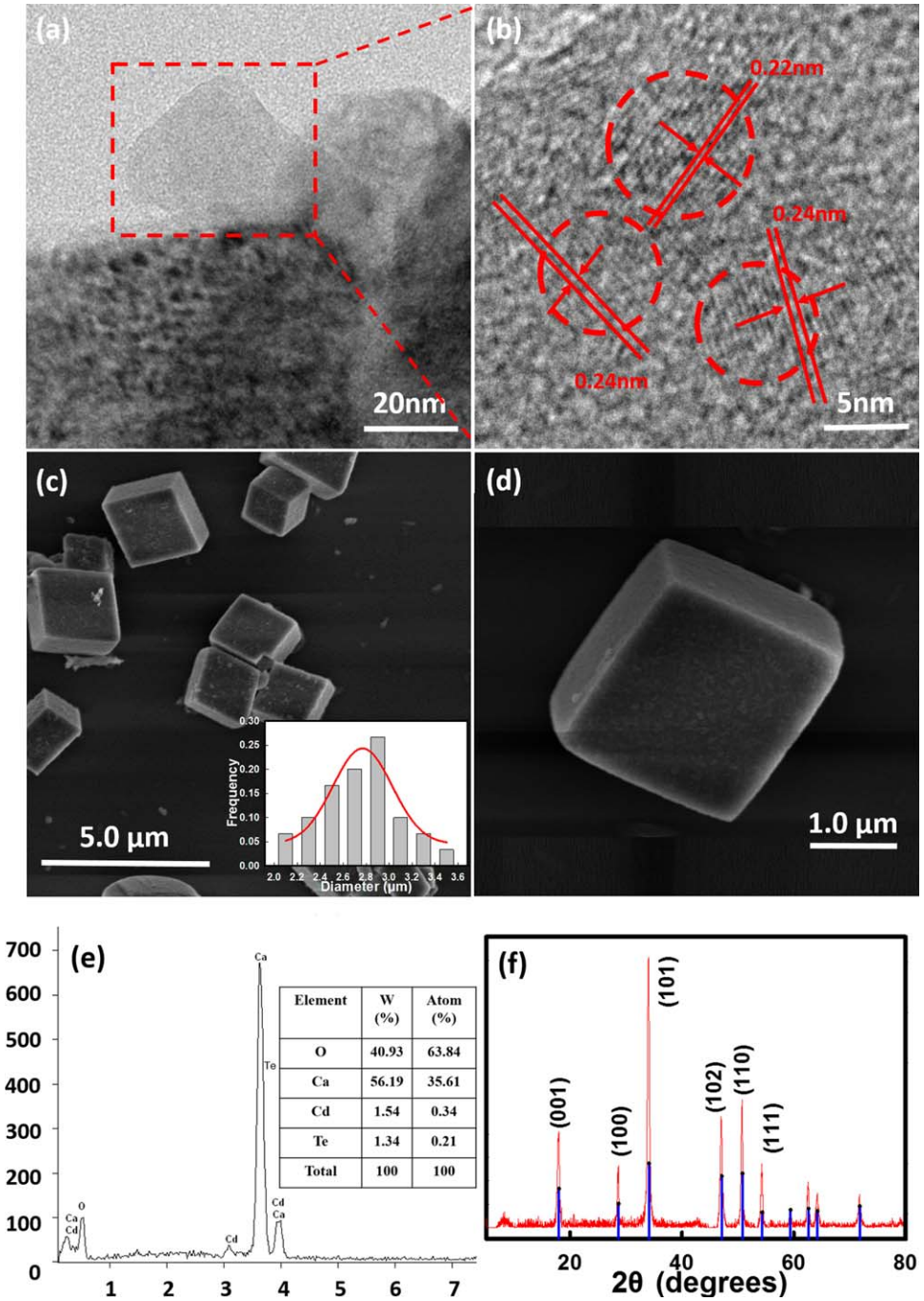

Figure 2. (a and b) TEM images of CdTe@Ca(OH)$_2$ nanocrystals and (b) is a HRTEM image; (c) SEM image of the CdTe@Ca(OH)$_2$ nanocrystals. The insert in (c) is the histogram of the particle size distribution; (d) Magnified SEM picture of a single particle; (e) EDX analysis of the CdTe@Ca(OH)$_2$ nanocrystals. Inset: a statistical table of all elements and the corresponding content; (f) XRD pattern of the CdTe@Ca(OH)$_2$ nanocrystals.

[Color figure can be viewed in the online issue, which is available at wileyonlinelibrary.com.]

were easily precipitated in the bottle of tube (seen in Figure 1d). To determine Cd^{2+} concentrations of CdTe QDs and CdTe@Ca(OH)$_2$ residual filtrates, we used ICP (Inductively Coupled Plasma) to detect them. The corresponding Cd^{2+} concentrations decreased from 1843.45 mg/L (CdTe QDs) to 0.238 mg/L (0.4 M CdTe@Ca(OH)$_2$). The Cd^{2+} concentration in the residual filtrate during the production process of CdTe@Ca(OH)$_2$ powders reaches as low as 0.238 ppm level, implying nearly all of the CdTe QDs are efficiently encapsulated into Ca(OH)$_2$ as well as the smallest harm of residual filtrate exists in this case.[33] wMoreover, the as-prepared CdTe@Ca(OH)$_2$ nanocrystal powder is of bright green fluorescence (emitted at 540 nm) and hexahedron structure (seen in Figure 1g). This finding may open an available pathway to facilely green synthesis of QDs powder with easily scaling up and high efficiency.

We further took TEM characterization to verify the encapsulation process (seen in Figures 2a, b). As indicated in Figure 2a, Ca(OH)$_2$ shell is too dense to allow electrons to penetrate CdTe@Ca(OH)$_2$ nanocrystals. After grinding CdTe@Ca(OH)$_2$

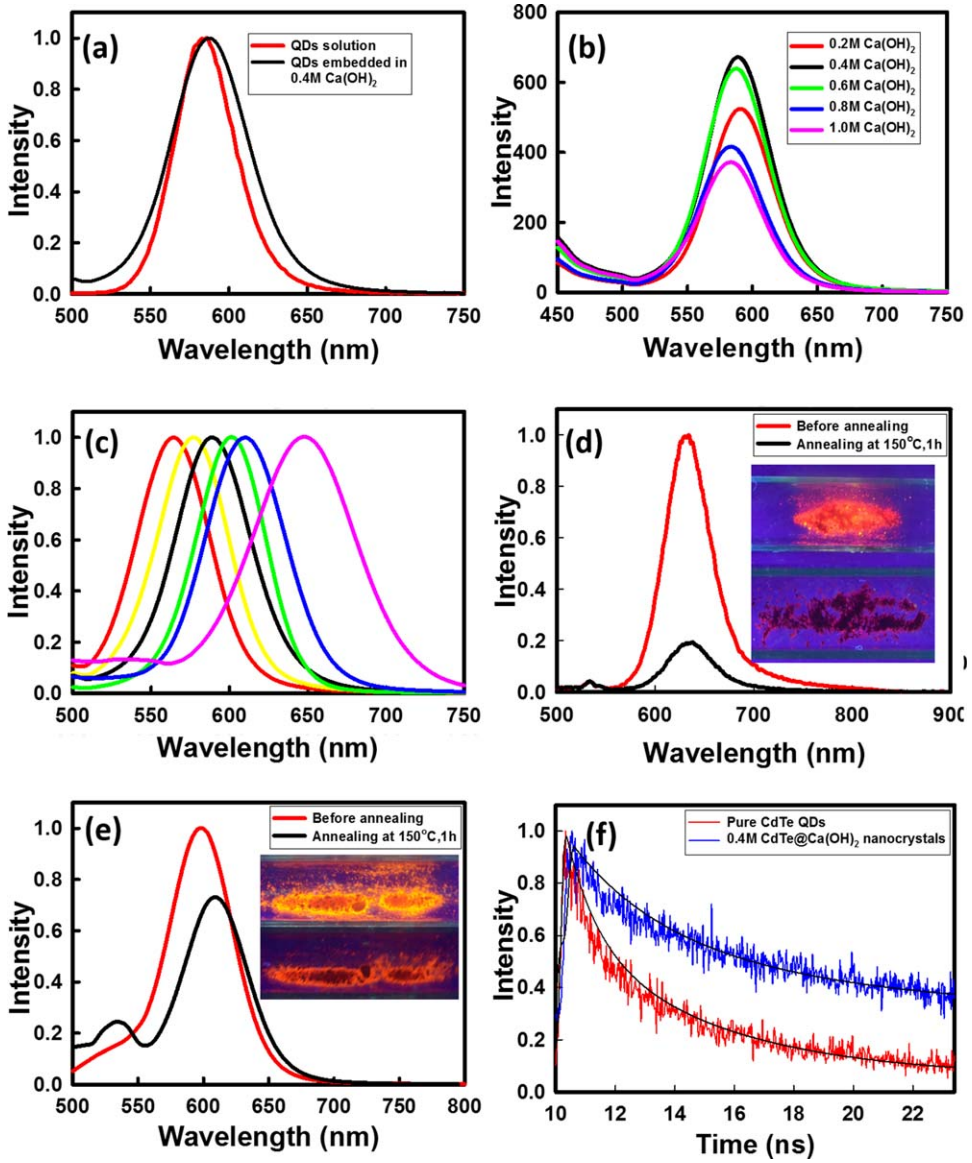

Figure 3. (a) Normalized PL spectra of QDs solution before and after embedding in $Ca(OH)_2$ crystals; (b) PL spectra of a series concentration of $Ca(OH)_2$, ranging from 0.2 to 1.0 M, with CdTe QDs embedded; (c) normalized PL spectra of QDs with different emission wavelength embedded in 0.4 M $Ca(OH)_2$; (d) PL spectra of QDs powder before and after annealing. Inset: corresponding fluorescent images before (upper) and after (down) annealing; (e) PL spectra of CdTe@$Ca(OH)_2$ nanocrystals before and after annealing. Inset: corresponding fluorescent images before (upper) and after (down) annealing; (f) time-resolved PL decay curves of CdTe QDs and 0.4 M CdTe@$Ca(OH)_2$ nanocrystals. The black lines are corresponding fitting curves of them.

[Color figure can be viewed in the online issue, which is available at wileyonlinelibrary.com.]

sample into smaller particle size with the Planetary Ball Mill, well-dispersed lattice fringes of CdTe nanocrystals are still obviously observed in the hybrid crystal as well as their lattice spacings are 0.22, 0.24, and 0.24 nm, corresponding to the (220) plane of cubic CdTe (seen in Figure 2b). Figures 2c, d present the typical SEM images of the CdTe@$Ca(OH)_2$ nanocrystals and the inset in Figure 2c is a histogram of the particle size distribution. The histogram manifests a relatively narrow size distribution with an average size of 2.8 μm. Figure 2d is a magnified SEM picture of a single particle, from which we can see that the $Ca(OH)_2$ crystals are typical hexahedron. The EDX analysis of the CdTe@$Ca(OH)_2$ nanocrystals demonstrates the existence of CdTe QDs and $Ca(OH)_2$. The EDX result in Figure 2e does not contain the peak of Te, which might be overlapped with the peak of Ca.[21] The inset in Figure 2e is a statistical table of all elements and the corresponding content. The XRD pattern is also shown in Figure 2f, and we can see the crystal structure fits well with the crystalline $Ca(OH)_2$ (portlandite).[34] The peaks of the XRD results are assigned to the (001), (100), (101), (102), (110), and (111) planes of the bulk portlandite.

We investigated PL properties of CdTe QDs solution and the CdTe@$Ca(OH)_2$ nanocrystals. As shown in Figure 3a, the emission wavelength of CdTe@$Ca(OH)_2$ exists nearly 7 nm red-shift comparing with that of CdTe QDs, which can be explained by changes of the dielectric constant of the

Table 1. PL Lifetimes of CdTe@$Ca(OH)_2$ Crystals with Different Concentrations

Parameters	1#	2#	3#	4#	5#	6#
$CaCl_2$ (mol/L)	0	0.2	0.4	0.6	0.8	1.0
NaOH (mol/L)	0	0.4	0.8	1.2	1.6	2.0
PL lifetime (ns)	4.37	5.69	7.89	8.86	9.58	11.37

surrounding media as well as by reabsorption of the emission from small nanocrystals by larger ones.[23,35,36] Figure 3b is PL spectra of CdTe@$Ca(OH)_2$ under different concentrations of $Ca(OH)_2$. As expected, there exists a optimal concentration of $Ca(OH)_2$ (0.4 M) to obtain highest PL intensity of nanocrystals. As the concentration of $Ca(OH)_2 < 0.4$ M, the concentrations of CdTe QDs are relatively higher, allowing their fluorescence weak due to occurrence of self-absorption.[37–40] Otherwise, when the concentration of $Ca(OH)_2 > 0.4$ M, it would reduce the concentrations of CdTe QDs, leading to lowering their fluorescence either. As such, we further synthesized CdTe@$Ca(OH)_2$ nanocrystals with different emission wavelengths under 0.4 M concentration of $Ca(OH)_2$ (seen in Figure 3c).

Comparison of the thermostability and PL lifetime between pure CdTe QDs and the CdTe@$Ca(OH)_2$ nanocrystals

By contrast CdTe@$Ca(OH)_2$ thermostability with CdTe QDs control sample, both samples were kept in a tube furnace at 150°C for 1 h, and then we measured PL spectra toward both

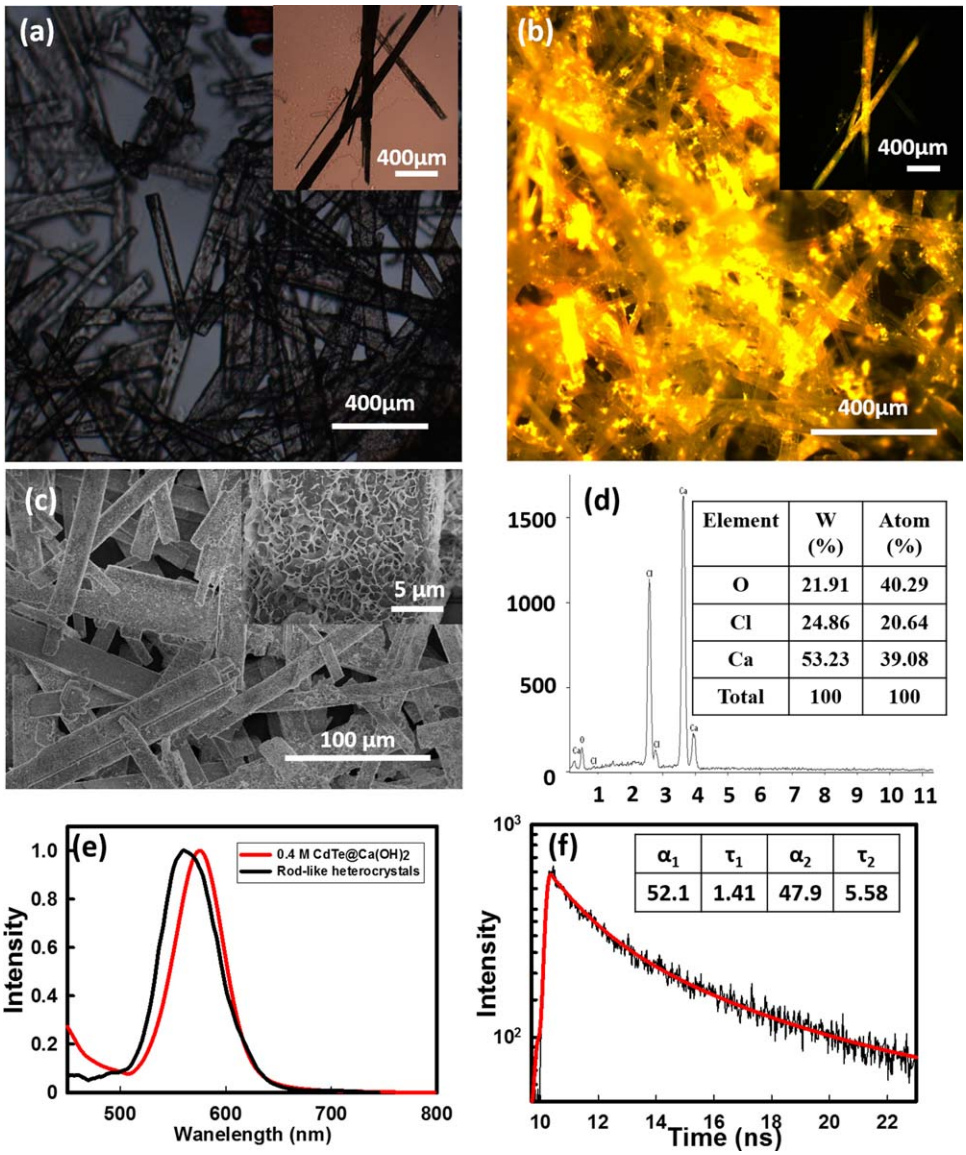

Figure 4. (a) Microscope image of the heterocrystals under irradiation of visual light; (b) fluorescent microscope image of the heterocrystals under irradiation of UV light. The insets in (a and b) are the corresponding magnified images of them. (c) SEM image of the heterocrystals and the inset is a magnified SEM image of the heterocrystals; (d) EDX results of the heterocrystals and the inset in it is the content of each element; (e) normalized PL spectra of 0.4 M CdTe@$Ca(OH)_2$ nanocrystals and rod-like heterocrystals; (f) time-resolved PL decay curve of the heterocrystals measured by laser confocal microscopy. The inset table is the corresponding fitting parameters and the red line is the fitting curve.

[Color figure can be viewed in the online issue, which is available at wileyonlinelibrary.com.]

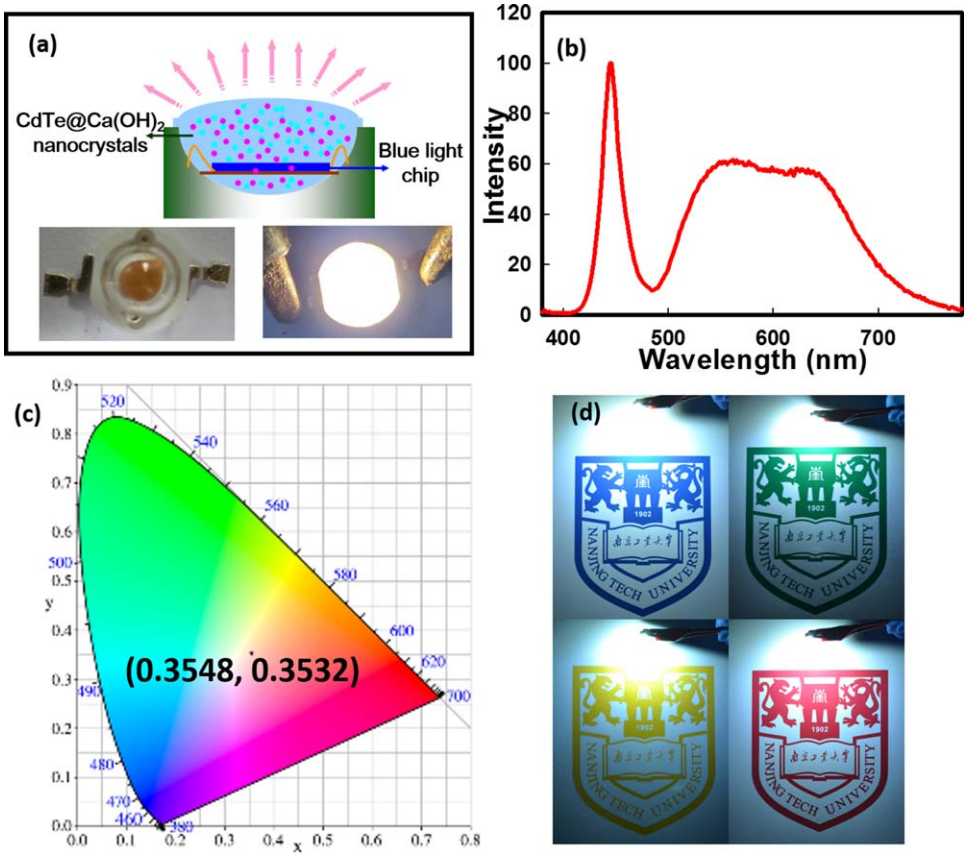

Figure 5. (a) Schematic diagram (upper) of the fabricated WLED and the actual product (down) manufactured by this schema; (b) emission spectrum of the WLED; (c) CIE chromaticity coordinate of the WLED.; (d) photographs of the WLED lighting pictures.

[Color figure can be viewed in the online issue, which is available at wileyonlinelibrary.com.]

samples at same time. Figures 3d, e are PL spectra of CdTe QDs powder (3d) and CdTe@$Ca(OH)_2$ (3e) nanocrystals ($Ca(OH)_2 = 0.4$ M) before and after annealing. As displayed in Figure 3d, for CdTe QDs powder, its fluorescent intensity has quenched 80% after annealing. However, for CdTe@-$Ca(OH)_2$ powder, its fluorescent intensity has quenched only 30% after annealing (Figure 3e). By contrast the thermostability of two samples, the thermostability of CdTe@-$Ca(OH)_2$ is 2.6 times better than that of CdTe QDs powder. This also indicates the thermostability of QDs after their embedding in $Ca(OH)_2$ crystal is highly enhanced because $Ca(OH)_2$ crystals are of good stability on the atmosphere. As expected, there exists red shift noted at the peak of emission spectrum of the CdTe@$Ca(OH)_2$ after the annealing. It could be explained by that the high temperature would induce further CdTe QDs growth in CdTe@$Ca(OH)_2$ nanocrystals. The fluorescent images of above two samples before (upper) and after annealing (down) (insert in Figures 3d, e) are consistent with the result of corresponding PL spectra, showing similar quenching trend after annealing.

We further investigated the PL lifetimes of CdTe QDs powder and CdTe@$Ca(OH)_2$. As indicated in Figure 3f, the decay traces of them are both biexponential and can be well fitted with the exponential function $Y(t)$ based on nonlinear least-square, using the following expression

$$Y(t) = \alpha_1 \exp(-t/\tau_1) + \alpha_2 \exp(-t/\tau_2) \quad (1)$$

in this equation α_1, α_2 are fractional contributions of time-resolved decay lifetimes τ_1, τ_2.[31,41] The black lines in Figure 3f are corresponding fitting curves of them. The average lifetime τ could be concluded from the Eq. 2

$$\bar{\tau} = \frac{\alpha_1 \tau_1^2 + \alpha_2 \tau_2^2}{\alpha_1 \tau_1 + \alpha_2 \tau_2} \quad (2)$$

As depicted in Figure 3f, the decay trace of the CdTe@-$Ca(OH)_2$ nanocrystals shows more flat fading tendency than that of pure CdTe QDs. The PL lifetime τ of the CdTe@-$Ca(OH)_2$ ($Ca(OH)_2 = 0.4$ M) nanocrystals ($\tau = 7.89$ ns) is much longer than that of pure CdTe QDs ($\tau = 4.37$ ns). The PL lifetimes with different concentrations of $Ca(OH)_2$ (0.2, 0.4, 0.6, 1.0 M) are summarized in Table 1. The date of 0 M represents the pure CdTe QDs. The PL lifetime appears longer as the increasing of the concentration of $Ca(OH)_2$. That result suggests that there exists the enhanced surface passivation effect when the concentrations of $Ca(OH)_2$ increase from 0 to 1.0 M, preventing aggregation of QDs, further causing the prolonging of the PL lifetime.[23]

Growth of the CdTe@$Ca(OH)_2$ nanocrystals into fluorescent rod-like heterocrystals

Perhaps more interestingly, when the as-prepared 2 g dried CdTe@$Ca(OH)_2$ nanocrystals were further soaked in 10 mL saturated $CaCl_2$ solution, the heterocrystal microwires were emerged (shown in Figures 4a–c). As saturated $CaCl_2$ solution is easily to separate crystals out with linear structure when pouring dried CdTe@$Ca(OH)_2$ nanocrystals in the solution. As shown in Figures 4a, c, the heterocrystals are well

dispersed and the average diameter of these microwires is about 50μm. Under UV light, they present bright yellow fluorescence (seen in Figure 4b). The EDX results also present the main components in the heterocrystals are $CaCl_2$ and $Ca(OH)_2$ compounds. (seen in Figure 4d). We also applied laser confocal microscopy to measure the PL spectrum and the PL lifetime of the heterocrystals. Figure 4e is the normalized PL spectra of CdTe@$Ca(OH)_2$ nanocrystals (0.4 M) and the rod-like heterocrystals. As shown in the PL spectra, there is blue-shift of emission peak noted from 575 to 561 nm occurs due to the decrease of the content of CdTe QDs in rod-like heterocrystals. Figure 4f is the time-resolved PL decay curve of the heterocrystals, corresponding the calculated PL lifetime of the heterocrystals is 4.93 ns.

Applications of CdTe@Ca(OH)$_2$ nanocrystals on WLED

The construction of WLED with QDs has drawn much attention owing to that this strategy has obvious advantage of excellent CRI comparing with traditional phosphor.[42] Although much approaches have been developed, the breakthrough in enhancement of QDs stability is still high expectation. Based on the fact that the CdTe@$Ca(OH)_2$ powders are easily to produce with large-scale and their PL stability have as 2.6 times as that of CdTe QDs powder, we utilize CdTe@$Ca(OH)_2$ as the phosphor to prepare WLED lamp (Figure 5a). The emission spectrum for the WLED, depicted in Figure 5b, shows three peaks centred at 450 nm, 560 nm and 625 nm, corresponding to the emission of blue light chip and two kinds of CdTe@$Ca(OH)_2$ nanocrystals with different emission wavelength, respectively. As seen in Figure 5c, the as-prepared WLED presents excellent properties, such as the CIE chromaticity coordinate (0.3548, 0.3532), high color temperature of 4643 K, CRI of 82.4 at the current of 350 mA. This WLED lamp could be applied to illuminate different color pictures with good performance (seen in Figure 5d).

Conclusions

In summary, we report a strategy for creating a series of CdTe@$Ca(OH)_2$ nanocrystals via a coprecipitation method, which present high production efficiency and good PL stability. The procedure of capping CdTe QDs into $Ca(OH)_2$ crystals is simple, green, and easily scaling-up, allowing the products to be easily filtrating separation and the Cd^{2+} ions content of residual filtrate solution to be reached to 0.238 ppm level. By contrast the thermostability of CdTe@$Ca(OH)_2$ with CdTe QDs, the thermostability of CdTe@$Ca(OH)_2$ is 2.6 times better than that of CdTe QDs powder as well as the PL lifetime is also greatly prolonged. We further construct fluorescent rod-like heterocrystals by addition of saturated $CaCl_2$ solution. More importantly, we applied stable CdTe@$Ca(OH)_2$ powders as phosphors to construct WLED with good CIE and CRI properties. Thus, more practical applications to this matter would continue and follow.

Acknowledgments

This work was supported by the National Natural Science Foundation of China (21006046 and 21474052), Natural Science Foundation of Jiangsu Province (BK20131408), and Priority Academic Program Development of Jiangsu Higher Education Institutions (PAPD).

Literature Cited

1. Medintz IL, Uyeda HT, Goldman ER, Mattoussi H. Quantum dot bioconjugates for imaging, labelling and sensing. *Nat Mater*. 2005; 4(6):435–446.
2. Peng ZA, Peng X. Formation of high-quality CdTe, CdSe, and CdS nanocrystals using CdO as precursor. *J Am Chem Soc*. 2001;123(1): 183–184.
3. Yin Y, Alivisatos AP. Colloidal nanocrystal synthesis and the organic-inorganic interface. *Nature*. 2005;437(7059):664–670.
4. Tang J, Kemp KW, Hoogland S, Jeong KS, Liu H, Levina L, Furukawa M, Wang X, Debnath R, Cha D, Chou KW, Fischer A, Amassian A, Asbury JB, Sargent EH. Colloidal-quantum-dot photovoltaics using atomic-ligand passivation. *Nat Mater*. 2011;10(10): 765–771.
5. Klimov VI, Mikhailovsky AA, Xu S, Malko A, Hollingsworth JA, Leatherdale CA, Eisler H, Bawendi MG. Optical gain and stimulated emission in nanocrystal quantum dots. *Science*. 2000;290(5490):314–317.
6. Dabbousi BO, Bawendi MG, Onitsuka O, Rubner MF. Electroluminescence from CdSe quantum-dot polymer composites. *Appl Phys Lett*. 1995;66(11):1316–1318.
7. Colvin VL, Schlamp MC, Alivisatos AP. Light-emitting-diodes made from cadmium selenide nanocrystals and a semiconducting polymer. *Nature*. 1994;370(6488):354–357.
8. Bruchez M, Jr. Semiconductor nanocrystals as fluorescent biological labels. *Science*. 1998;281(5385):2013–2016.
9. Schaller RD, Klimov VI. High efficiency carrier multiplication in PbSe nanocrystals: implications for solar energy conversion. *Phys Rev Lett*. 2004;92(18):186601.
10. Murray CB, Norris DJ, Bawendi MG. Synthesis and characterization of nearly monodisperse CdE (E = sulfur, selenium, tellurium) semiconductor nanocrystallites. *J Am Chem Soc*. 1993;115(19):8706–8715.
11. Yu WW, Peng X. Formation of high-quality CdS and other II-VI semiconductor nanocrystals in noncoordinating solvents: tunable reactivity of monomers. *Angew Chem Int Ed Engl*. 2002;41(13): 2368–2371.
12. Pan J, Wan D, Bian Y, Guo Y, Jin F, Wang T, Gong J. Reduction of nonspecific binding for cellular imaging using quantum dots conjugated with vitamin E. *AlChE J*. 2014;60(5):1591–1597.
13. Maroudas D, Han X, Pandey SC. Design of semiconductor ternary quantum dots with optimal optoelectronic function. *AlChE J*. 2013; 59(9):3223–3236.
14. Gattas-Asfura KM, Leblanc RM. Peptide-coated CdS quantum dots for the optical detection of copper(II) and silver(I). *Chem Commun*. 2003;(21):2684.
15. Gerion D, Pinaud F, Williams SC, Parak WJ, Zanchet D, Weiss S, Alivisatos AP. Synthesis and properties of biocompatible water-soluble silica-coated CdSe/ZnS semiconductor quantum dots. *J Phys Chem B*. 2001;105(37):8861–8871.
16. Hou L, Zhang Q, Ling L, Li CX, Chen L, Chen S. Interfacial fabrication of single-crystalline ZnTe nanorods with high blue fluorescence. *J Am Chem Soc*. 2013;135(29):10618–10621.
17. Hou L, Chen L, Chen S. Interfacial self-assembled fabrication of petal-like CdS/dodecylamine hybrids toward enhanced photoluminescence. *Langmuir*. 2009;25(5):2869–2874.
18. Rejinold NS, Baby T, Nair SV, Jayakumar R. Paclitaxel loaded fibrinogen coated CdTe/ZnTe Core shell nanoparticles for targeted imaging and drug delivery to breast cancer cells. *J Biomed Nanotechnol*. 2013;9(10):1657–1671.
19. Yong K-T, Roy I, Law W-C, Hu R. Synthesis of cRGD-peptide conjugated near-infrared CdTe/ZnSe core–shell quantum dots for in vivo cancer targeting and imaging. *Chem Commun*. 2010;46(38): 7136.
20. Bae WK, Kwak J, Park JW, Char K, Lee C, Lee S. Highly efficient green-light-emitting diodes based on CdSe@ZnS quantum dots with a chemical-composition gradient. *Adv Mater*. 2009;21(17):1690–1694.
21. Hu L, Mao Z, Gao C. Fabrication of fluorescent microparticles by doping water-soluble CdTe nanocrystals into calcium carbonate for monitoring intracellular uptake. *Colloids Surf Physicochem Eng Asp*. 2009;336(1-3):115–122.
22. Yang P, Murase N. Preparation-condition dependence of hybrid SiO2-coated CdTe nanocrystals with intense and tunable photoluminescence. *Adv Funct Mater*. 2010;20(8):1258–1265.
23. Chang Y, Yao X, Zhang Z, Jiang D, Yu Y, Mi L, Wang H, Li G, Yu D, Jiang Y. Preparation of highly luminescent BaSO4protected CdTe quantum dots as conversion materials for excellent color-rendering white LEDs. *J Mater Chem C*. 2015;3(12):2831–2836.

24. Wolcott A, Gerion D, Visconte M, Sun J, Schwartzberg A, Chen S, Zhang JZ. Silica-coated CdTe quantum dots functionalized with thiols for bioconjugation to IgG proteins. *J Phys Chem B*. 2006; 110(11):5779–5789.
25. Sadaf A, Zeshan B, Wang Z, Zhang R, Xu S, Wang C, Cui Y. Toxicity evaluation of hydrophilic CdTe Quantum Dots and CdTe@SiO_2 nanoparticles in mice. *J Nanosci Nanotechnol*. 2012;12(11):8287–8292.
26. Zhu L, Xu L, Wang J, Yang S, Wang C-F, Chen L, Chen S. Macromonomer-induced CdTe quantum dots toward multicolor fluorescent patterns and white LEDs. *RSC Adv*. 2012;2(24):9005–9010.
27. Zhang H, Wang LP, Xiong HM, Hu LH, Yang B, Li W. Hydrothermal synthesis for high-quality CdTe nanocrystals. *Adv Mater*. 2003; 15(20):1712-+.
28. Zhao D, Fang Y, Wang H, He Z. Synthesis and characterization of high-quality water-soluble CdTe: Zn2+ quantum dots capped by N-acetyl-l-cysteine via hydrothermal method. *J Mater Chem*. 2011; 21(35):13365.
29. Li C-X, Yu C, Wang C-F, Chen S. Facile plasma-induced fabrication of fluorescent carbon dots toward high-performance white LEDs. *J Mater Sci*. 2013;48(18):6307–6311.
30. Duan JL, Song LX, Zhan JH. One-pot synthesis of highly luminescent CdTe quantum dots by microwave irradiation reduction and their Hg2+-sensitive properties. *Nano Res*. 2009;2(1):61–68.
31. Ling L, Zhu L, Zhang Q, Wang C-F, Chen S. Interface-spawned NiSe quantum dots: preparation, photoluminescence properties and applications. *J Mater Chem C*. 2014;3(2):473–478.
32. Wang W, Deng Z, Zhang Y, Wang C-F, Chen L, Chen S. Self-replication fabrication of ligand-free CdSe quantum dots on a nanofiber microreactor via a solid–liquid interfacial method. *Ind Eng Chem Res*. 2014;53(21):8753–8758.
33. Sharma RK, Mittal S, Azami S, Adholeya A. Surface modified silica gel for extraction of metal ions: an environment friendly method for waste treatment. *Surf Eng*. 2005;21(3):232–237.
34. Ambrosi M, Dei L, Giorgi R, Neto C, Baglioni P. Colloidal particles of Ca(OH)2: properties and applications to restoration of frescoes. *Langmuir*. 2001;17(14):4251–4255.
35. Otto T, Müller M, Mundra P, Lesnyak V, Demir HV, Gaponik N, Eychmüller A. Colloidal nanocrystals embedded in macrocrystals: robustness, photostability, and color purity. *Nano Lett*. 2012;12(10): 5348–5354.
36. Koole R, Liljeroth P, de Mello Donegá C, Vanmaekelbergh D, Meijerink A. Electronic coupling and exciton energy transfer in CdTe quantum-dot molecules. *J Am Chem Soc*. 2006;128(32): 10436–10441.
37. Mueller AH, Petruska MA, Achermann M, Werder DJ, Akhadov EA, Koleske DD, Hoffbauer MA, Klimov VI. Multicolor light-emitting diodes based on semiconductor nanocrystals encapsulated in GaN charge injection layers. *Nano Lett*. 2005;5(6): 1039–1044.
38. Wang F, Kreiter M, He B, Pang S, Liu CY. Synthesis of direct white-light emitting carbogenic quantum dots. *Chem Commun*. 2010; 46(19):3309–3311.
39. Dang C, Lee J, Breen C, Steckel JS, Coe-Sullivan S, Nurmikko A. Red, green and blue lasing enabled by single-exciton gain in colloidal quantum dot films. *Nat Nanotechnol*. 2012;7(5):335–339.
40. Wang X, Yan X, Li W, Sun K. Doped quantum dots for white-light-emitting diodes without reabsorption of multiphase phosphors. *Adv Mater*. 2012;24(20):2742–2747.
41. Yang S, Wang CF, Chen S. Interface-directed assembly of one-dimensional ordered architecture from quantum dots guest and polymer host. *J Am Chem Soc*. 2011;133(22):8412–8415.
42. Anikeeva PO, Halpert JE, Bawendi MG, Bulovic V. Electroluminescence from a mixed red-green-blue colloidal quantum dot monolayer. *Nano Lett*. 2007;7(8):2196–2200.

Manuscript received Sep. 16, 2015, and revision received Nov. 7, 2015.